Characterization of Phosphate Sequestration by a Lanthanum Modified Bentonite Clay: A Solid-State NMR, EXAFS, and PXRD Study

ARTICLE *in* ENVIRONMENTAL SCIENCE AND TECHNOLOGY · MARCH 2015

Impact Factor: 5.33 · DOI: 10.1021/es506182s · Source: PubMed

6 AUTHORS, INCLUDING:

Andrew S Lipton
Pacific Northwest National Laboratory
55 PUBLICATIONS **1,032** CITATIONS
SEE PROFILE

Kasper Reitzel
University of Southern Denmark
37 PUBLICATIONS **714** CITATIONS
SEE PROFILE

T. E. Warner
University of Southern Denmark
35 PUBLICATIONS **183** CITATIONS
SEE PROFILE

Ulla Gro Nielsen
University of Southern Denmark
33 PUBLICATIONS **589** CITATIONS
SEE PROFILE

Environmental Science & Technology

Article

pubs.acs.org/est

Characterization of Phosphate Sequestration by a Lanthanum Modified Bentonite Clay: A Solid-State NMR, EXAFS, and PXRD Study

Line Dithmer,[†,‡] Andrew S. Lipton,[§] Kasper Reitzel,[‡] Terence E. Warner,[∥] Daniel Lundberg,[⊥] and Ulla Gro Nielsen*[,†]

[†]Department of Physics, Chemistry, and Pharmacy, University of Southern Denmark, 5230 Odense M, Denmark

[‡]Department of Biology, University of Southern Denmark, 5230 Odense M, Denmark

[§]Environmental Molecular Sciences Laboratory, Pacific Northwest National Laboratory, 902 Battelle Boulevard, Richland, Washington 99354, United States

[∥]Department of Chemical Engineering, Biotechnology and Environmental Technology, University of Southern Denmark, Niels Bohrs Allé 1, 5230 Odense M, Denmark

[⊥]Department of Chemistry and Biotechnology, Uppsala BioCenter, Swedish University of Agricultural Sciences, P.O. Box 7015, SE-750 07 Uppsala, Sweden

Supporting Information

ABSTRACT: Phosphate (P_i) sequestration by a lanthanum (La) exchanged clay mineral (La-Bentonite), which is extensively used in chemical lake restoration, was investigated on the molecular level using a combination of ^{31}P and ^{139}La solid state NMR spectroscopy (SSNMR), extended X-ray absorption spectroscopy (EXAFS), powder X-ray diffraction (PXRD) and sorption studies. ^{31}P SSNMR show that all P_i was immobilized as rhabdophane ($LaPO_4{\cdot}n\ H_2O$, $n \leq 3$), which was further supported by ^{139}La SSNMR and EXAFS. However, PXRD results were ambiguous with respect to rhabdophane and monazite ($LaPO_4$). Adsorption studies showed that at dissolved organic carbon (DOC) concentration above ca. 250 μM the binding capacity was only 50% of the theoretical value or even less. No other La or P_i phases were detected by SSNMR and EXAFS indicating the effect of DOC is kinetic. Moreover, ^{31}P SSNMR showed that rhabdophane formed upon P_i sequestration is in close proximity to the clay matrix.

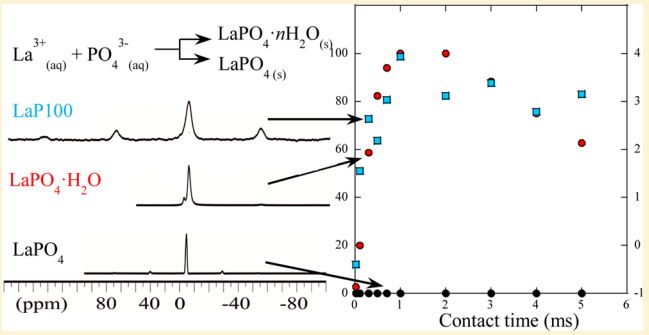

INTRODUCTION

Eutrophication of freshwater lakes is a worldwide problem, and in Europe more than 35% (32 000 km^2) of the total lake area fails to fulfill the 2015 target set by the European Water Framework Directive (WFD) (EC2000/60/EC).[1] The main reason is decades of external phosphorus (P) inputs to lakes from urban and agricultural sources causing accumulation of P in the sediments. A large part of this P pool is mobile and contains P bound to oxidized iron (Fe(III)) as well as organic bound P.[2] Hence, mineralization of organic matter leads to P release from the organic bound P pool during the summer. High mineralization rates often cause anoxic conditions resulting in a reduction of Fe(III) to Fe(II) and thereby a remobilization of the iron bound P. This P release from the mobile P pool can consequently support a high in-lake concentration of phytoplankton leading to turbid water.

There are several strategies for remediation of P polluted lakes including oxygenation of Fe containing sediment,[3] dredging,[4,5] and addition of chemicals such as Fe, aluminum (Al), and Phoslock.[5−10] Addition of P binding chemicals to combat eutrophication in lakes is termed "chemical lake restoration" and aims to immobilize excess P via chemical reactions and formation of insoluble stable phosphate minerals.[11] These are subsequently incorporated in the lake sediment and leaves P unavailable for primary producers. Al(III) ions are commonly used for restoring the natural level of P in the lakes. However, it should not be used in soft water lakes, lakes in risk of high pH, or shallow lakes, with high resuspension potential due to the acidic properties of Al(III) ions.[8,12,13]

Newer solutions and products targeting an optimized environmental remediation are continuously being developed. Therefore, studies to assess the pros and cons of these new products are needed to determine the optimum remediation strategy. One of these recent products is Phoslock, a commercial bentonite clay product, developed by CSIRO, Australia,[6] and with lanthanum (La) ion-exchanged to a

Received: December 19, 2014
Revised: March 5, 2015
Accepted: March 6, 2015
Published: March 6, 2015

DOI: 10.1021/es506182s
Environ. Sci. Technol. 2015, 49, 4559−4566

concentration of 4.4 w/w%.[14,15] The uses of chemically modified clays has increased and they are now among the main commercial restoration products in Europe. Given the frequent use of Phoslock it is essential to extend the knowledge about phosphate (P_i) sequestration to the molecular scale, e.g., identify the chemical composition of the stable biounavailable P phase(s) formed and the effects of parameters such as pH, alkalinity, and humic acids on the binding capacity and time scale of P removal.

The ion-exchanged La in Phoslock captures and immobilizes P as an insoluble La phosphate phase.[6,16] There are several known La phosphate phases including two La orthophosphate polymorphs, the anhydrous monazite ($LaPO_4$), and the hydrous rhabdophane ($LaPO_4{\cdot}n\ H_2O$, $n \leq 3$).[17−20] The two orthophosphates differ in their crystal structure, as rhabdophane is hexagonal with 1D channels along the *c*-axis containing zeolitic water, whereas the anhydrous monazite has a more condensed monoclinic structure (Supporting Information (SI), Figure SI-1).[18,21] The reported binding capacity of Phoslock is one metric ton of Phoslock to capture 11 kg of P_i,[22] but other studies have found evidence for competitive bindings of oxyanions, such as carbonates and humic substances to La, which reduces the P_i binding capacity.[7,14,23−25] Moreover, dissolved organic carbon (DOC) can possibly form complexes with La(III),[5,26,27] and because La phosphate is difficult to characterize due to low concentrations in the clay matrix, little is known about the molecular level structure of the P binding and potential interference from other species such as carbonates and DOC. This information is crucial to assess the long-term stability of the P_i removal.

Solid state NMR spectroscopy (SSNMR) is a versatile technique for studies of environmental samples and provides information about different phases.[28,29] ^{31}P SSNMR is widely used to obtain information on environmental samples,[30] for example detailed information about the binding of phosphate on iron oxyhydroxides,[31] gibbsite and kaolinite[32] as well as Al oxides,[33,34] the latter, in a combination with ^{27}Al and ^{1}H SSNMR. In contrast, ^{139}La SSNMR spectra are often hundreds of kHz or several MHz wide due to a large quadrupole moment, making it much more challenging than, e.g., ^{31}P NMR. Thus, ^{139}La SSNMR studies have not been reported for environmental samples to our knowledge, although a few earlier studies have provided structural information about inorganic materials.[35−38]

To complement SSNMR, the local atomic structure around the La(III) ion is determined using La L_{III}-edge extended X-ray absorption fine structure (EXAFS) spectroscopy. EXAFS has previously been used for characterization of rare earth elements and their sorption onto and retention by clays,[39,40] in addition probing interactions among various ions, humic substances, and clays.[41,42] However, to our knowledge, little information is available about the local structure after ion-exchange of rare earth elements within the clay structure and reactions with dissolved phosphate, except for a study of lanthanoid(III) ions intercalated in vermiculite.[43] Powder X-ray diffraction (PXRD) provides useful information about crystalline phases and has yet to be used in connection to sequestration by Phoslock.

The current study investigates P_i sequestration by Phoslock as a function of P_i loading and DOC concentration by SSNMR, EXAFS, and PXRD in combination with sorption experiments, as macroscopic observations cannot stand alone in investigating sorption mechanism and products. The objective is to achieve detailed insight into the speciation of the La phosphate phases in Phoslock.

EXPERIMENTAL SECTION

Materials and Reagents. The synthesis of the model compounds monazite ($LaPO_4$) and rhabdophane ($LaPO_4{\cdot}1.4H_2O$) is described in the SI (Appendix SI-1 and SI-2). Physical mixtures of rhabdophane and Fe(II) sulfate ($FeSO_4$;0.75 and 10 w/w%) were prepared by grinding the solids intimately in a mortar.

Adsorption Studies. *P_i Loading.* The effect of P_i loading was investigated by adding 0.7 g of Phoslock to 50 mL of water enriched with 0.01 M potassium hydrogen phosphate, K_2HPO_4, in concentrations corresponding to Phoslock:P_i (w/w) ratios of 300:1 (LaP300), 100:1 (LaP100), 50:1 (LaP50), and 25:1 (LaP25).

Humic Acid. The influence of DOC was tested with samples (triplicates) of Phoslock:P_i ratio 100:1 (the recommended dose) and humic acid (HA; Sigma-Aldrich, CAS 1415-93-6), as a model for DOC, at concentrations of 100 μM (LaP100-HA_{100}), 500 μM (LaP100-HA_{500}), and 1000 μM (LaP100-HA_{1000}). The pH was maintained at 6 for all samples, and they were shaken continuously for 1 week. The solid Phoslock phase was separated from the supernatant by centrifugation (5 min, 4000 rpm) and dried at room temperature. The samples were ground in a mortar before characterization by PXRD, NMR, and EXAFS.

Phosphate Sorption Experiments of Phoslock Samples. Water from Lake Hostrup, a shallow freshwater lake in Southern Denmark, was enriched with potassium hydrogen phosphate (K_2HPO_4) to a starting concentration of 20 μM to obtain concentrations mimicking eutrophic lakes (triplicates, 50 mL tubes, pH ∼6). Phoslock was added from a stock solution (0.6 mg L^{-1} Phoslock) and dosed in a ratio of 100:1 Phoslock:P_i (w/w). DOC was added to the samples in concentrations of 50, 100, 250, 500, and 1000 μM, representative values for Danish lakes.[44] Control samples without Phoslock were also analyzed. All samples were shaken continuously for 7 days followed by centrifugation to separate the Phoslock pellet and the supernatant. The latter was filtered and acidified (200 μL 2 M sulfuric acid pr. Five mL solution) to keep soluble reactive phosphate (SRP) in solution. The SRP concentrations in the supernatants were measured with a standard spectrophotometric method.[45]

Powder X-ray Diffraction. All samples were characterized with a Phillips PANanalytical PXRD diffractometer using Cu Kα radiation with λ = 1.5406 Å, in reflection-transmission mode and in the 2θ range 5−70°. The software X'Pert HighScore Plus 3.0 (PANanalytical B.V.) was used to match obtained diffractograms with the ICDD library.

Solid State NMR Spectroscopy. Solid state ^{31}P MAS NMR spectra were obtained on a Varian Inova 500 MHz spectrometer using a 3.2 mm double resonance MAS probe. Spinning speed ranged from 8 to 10 kHz, and the recycle delay was 60 s to ensure full relaxation for the Phoslock samples and 120−1000 s for the La phosphate model compounds. A spectrum of high quality was obtained for the Phoslock samples in a few hours using ca. 50 mg sample. Both single pulse ^{31}P NMR spectra with proton decoupling and ^{31}P{^{1}H} cross-polarization (CP) experiments were performed. ^{1}H MAS NMR spectra were recorded at 600 MHz using 1.6 mm triple resonance MAS probe and 35 kHz spinning. The ^{1}H and ^{31}P MAS NMR spectra were referenced relative to water (δ_{iso}(^{1}H)

DOI: 10.1021/es506182s
Environ. Sci. Technol. 2015, 49, 4559−4566

= 4.6 ppm) and 85% phosphoric acid ($\delta_{iso}(^{31}P)$ = 0 ppm), respectively, and analyzed using SpinWorks 3.1.8.1.[46]

Static ^{139}La NMR was performed at 21.1 T (127 MHz) for the Phoslock, samples, monazite and rhadophane using a home-built 5 mm static probe and the QCPMG sequence.[47] The spectra were referenced relative to a 1 M La(III) chloride solution ($\delta_{iso}(^{139}La)$ = 0 ppm). The complete spectrum was obtained by recording a series of subspectra due to a limited excitation bandwidth, and these subspectra were subsequently combined using a skyline projection. The carrier frequency was shifted in 50 kHz steps, and a total of 12−14 subspectra were recorded to ensure detection of the entire central transition. Typically, 50 000−100 000 scans per subspectra with a relaxation time of 0.3−3 s were accumulated, corresponding to 2−4 days of experiment time per spectrum. Selected spectra were recorded using WURST[48] for detection of the complete spectrum in a single experiment, as used earlier for ^{139}La.[37] ^{139}La NMR spectra were analyzed using the NMR simulation software SIMPSON,[49] which allowed for determination of the ^{139}La NMR parameters.

Extended X-ray Absorption Fine Structure. EXAFS measurements were performed at beamline I811, MAX-lab, Lund University, Sweden, which operates at 1.5GeV with a maximum ring current of 200 mA. The station was equipped with a Si[111] double crystal monochromator. Data collection was performed in fluorescence mode using ion chambers with stationary gas mixtures and a passivated implanted planar silicon (PIPS) detector. A titanium filter was used together with Soller slits to reduce fluorescence and scattering contributions. The monochromator was detuned to 60% of maximum intensity to reduce higher-order harmonics. The samples were ground and mounted with tape in aluminum frames, and five scans of 180 s for the 500 kV range were collected and averaged for each sample.

The EXAFS functions and parameters were extracted using standard procedures in the EXAFSPAK program package.[50] The standard deviations given for the refined parameters were obtained from k^3 weighted least-squares refinements of the EXAFS function $\chi(k)$ and do not include systematic errors of the measurements. These statistical error estimates provided a measure of the precision of the results and allow reasonable comparisons. An anomalous feature was observed in all spectra at k = 5−6 Å^{-1} due to double electron excitation, 2p4d → 5d^2, a phenomena commonly observed for all lanthanoids,[51] and a glitch at k = 8 Å. These were removed with the built-in deglitching function in EXAFSPAK. The k^3-weighted EXAFS functions were fitted toward scattering pathways calculated from theoretical models using FFEF7.[52]

RESULTS AND DISCUSSION

Identification of Crystalline Species by Powder X-ray Diffraction. The PXRD diffractogram of pure Phoslock contains only reflections from the clay matrix (bentonite), which also were observed for the phosphate samples with and without the presence of DOC (SI, Figure SI-2). Several weak and broad reflections appear after P_i sorption, which match the PXRD diffractograms of both monazite and rhabdophane, but further comparison is not possible. Moreover, no reflections from other crystalline phases such as La oxides or carbonates were observed, both for samples with and without DOC. Thus, the presence of DOC does not result in formation of new crystalline phases. The d-spacing is not changed for Phoslock, LaP100 and La100-HA$_{100}$, indicating that neither La phosphate nor DOC changed the crystal structure. Thus, PXRD identified a La phosphate phase, but whether this is a hydrous or anhydrous is ambiguous.

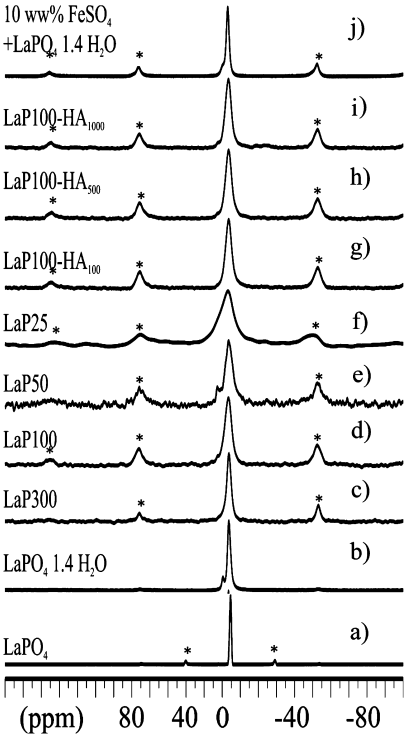

Figure 1. ^{31}P MAS NMR spectra of (a) $LaPO_4$, (b) $LaPO_4{\cdot}1.4H_2O$, and the seven Phoslock samples with (c) LaP300, (d) LaP100, (e) LaP50, (f) LaP25, (g) LaP100-HA$_{100}$, (h) LaP100-HA$_{500}$, (i) LaP100-HA$_{1000}$, and (j) LaPO4·1.4H$_2$O mixed with 10 w/w% $FeSO_4$. Asterisks denote ssbs.

Assignments and Quantifications of the Phosphate Species by ^{31}P MAS NMR. More detailed insight was obtained from ^{31}P MAS NMR spectroscopy. Figure 1 shows the ^{31}P MAS NMR spectra of the two La orthophosphates and the seven Phoslock samples. The results from the analysis of these spectra are summarized in Table 1. The ^{31}P MAS NMR spectra of monazite ($LaPO_4$; Figure 1a) and rhabdophane ($LaPO_4{\cdot}1.4H_2O$; Figure 1b) have the characteristic features of an orthophosphate: a strong isotropic resonance and a few very weak spinning side bands (ssbs) from the small chemical shift anisotropy (CSA). Monazite and rhabdophane can readily be distinguished based on their isotropic chemical shifts $\delta_{iso}(^{31}P)$, which are −4.58(0) and −3.47(1) ppm, respectively, c.f. Table 1, in agreement with earlier reported data.[20,53,54] The ^{31}P MAS NMR spectrum of rhabdophane (Figure 2b) has an additional resonance at $\delta_{iso}(^{31}P)$ = −0.48(8) ppm, which constitutes 9 % of the total intensity. Lucas et al.[55] proposed that the formula unit of rhabdophane should be $LaPO4{\cdot}nH_2O{\cdot}(H_3PO_4)_x$, $n \approx 0.5$, $0 < x < 0.1$ to accommodate phosphoric acid adsorbed on the surface, and similar $\delta_{iso}(^{31}P)$ were observed recently for phosphoric acid sorbed on niobium orthophosphates.[56] Thus, we assign this resonance to phosphoric acid on the surface of rhabdophane. It should be noted that $\delta_{iso}(^{31}P)$ reported for rhabdophane varies from −3.35 ppm to −3.8 ppm depending on the water content;[20,57] hence, a higher water content gives a $\delta_{iso}(^{31}P)$ shifted to lower shielding.

DOI: 10.1021/es506182s
Environ. Sci. Technol. 2015, 49, 4559−4566

Table 1. Isotropic Chemical Shift (δ_{iso}(^{31}P)) and Relative Intensity, When Applicable, Determined from Analysis of the ^{31}P MAS NMR Spectra, Shown in Figure 1

sample	δ_{iso}(^{31}P) (ppm)	rel. int. (%)
$LaPO_4$, PO_4^{3-}	−4.58(0)	100
$LaPO_4{\cdot}1.4H_2O$, PO_4^{3-}	−3.47(0)	90.6(6)
surface-P[a]	−0.45(8)	9.4(6)
$LaPO_4{\cdot}1.4H_2O$ +		
10 w/w% $FeSO_4$, PO_4^{3-}	−3.54(2)	88.1(8)
surface-P[a]	−0.31(12)	11.9(9)
$LaHP_2O_7{\cdot}3H_2O$[b]	−7.6	
	−16.9	
LaP300, PO_4^{3-}	−3.68(4)	100
surface-P[a]		
LaP100, PO_4^{3-}	−3.40(5)	91.7(3)
surface-P[a]	0.23(4)	8.3(0)
LaP50, PO_4^{3-}	−3.56(4)	84.9(7)
surface-P[a]	2.50(4)	15.1(7)
LaP25, PO_4^{3-}	−3.23(7)	80.7(3)
surface-P[a]	1.8(16)	19.3(3)
LaP100-HA_{100}, PO_4^{3-}	−3.39(2)	83.4(2)
surface-P[a]	−2.2(3)	16.6(2)
LaP100-HA_{500}, PO_4^{3-}	−3.23(8)	98.7(4)
surface-P[a]	2.71(5)	1.3(4)
LaP100-HA_{1000}, PO_4^{3-}	−3.24(4)	88.2(2)
surface-P[a]	−1.68(7)	11.4(2)

[a]Surface-P is mobile P-species formed on $LaPO_4{\cdot}nH_2O$ [b]Data reported by Ben Moussa et al.[58]

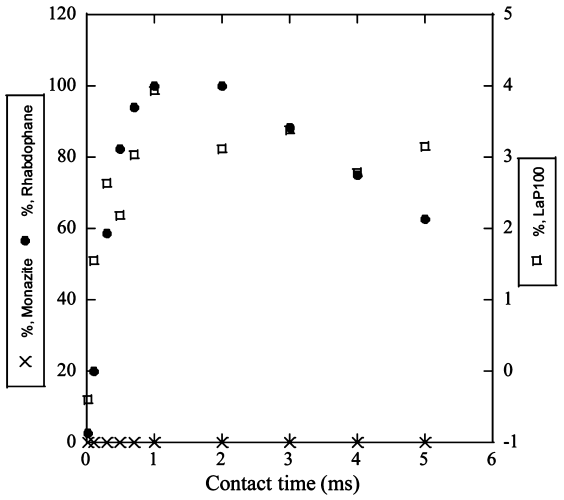

Figure 2. Relative intensities of rhabdophane ($LaPO_4$ 1.4 H_2O) (●), monazite ($LaPO_4$) (×), and LaP100 (□) determined from ^{31}P{^{1}H} CP MAS NMR experiments as a function of contact time. The intensities are normalized relative to the most intense value for rhabdophane (1 ms).

The ^{31}P MAS NMR spectra of the seven Phoslock samples (Figure 1c–i) show δ_{iso}(^{31}P) values in the chemical shift region observed for rhabdophane and a shoulder from phosphoric acid on the surface (Table 1, and SI, Figure SI-3). However, the overall ^{31}P MAS NMR spectrum does not look like that of rhabdophane, as several intense ssbs are observed for the Phoslock samples in contrast to the pure rhabdophane (Figure 1b). Normally, such intense ssbs would be caused by large CSA, but this is very unusual for orthophosphates. Moreover, the observed δ_{iso}(^{31}P) does not match those reported for La pyrophosphate[58](see Table 1), thus eliminating the possibility for other P phases. Paramagnetic ions can give rise to intense ssbs in SSNMR studies of clays[59] and humic acids,[60] and Phoslock contains about 0.75 w/w% Fe.[14] To verify this, physical mixtures of 0.75 and 10 w/w% $FeSO_4$ and rhabdophane were prepared, and these sample mixtures had ^{31}P MAS NMR spectra very similar to that of Phoslock, as illustrated in Figure 1j for 10 w/w% $FeSO_4$. Moreover, the relaxation times of the Phoslock samples were reduced by a factor of 2 as compared to pristine rhabdophane, an additional indicator of interactions with paramagnetic ions. Thus, we conclude that the intense ssbs in Phoslock are caused by the presence of paramagnetic ions and that the rhabdophane phase is in close proximity to the clay.

The ^{31}P MAS NMR spectra of the Phoslock samples are very similar, indicating that changing neither La:P ratio (LaP300, LaP100, LaP50, and LaP25) nor DOC (LaP100-HA_{100}, LaP100-HA_{500}, and LaP100-HA_{1000}) have an influence on the P phase because rhabdophane, with multiple ssbs caused by paramagnetic Fe in the clays, was observed for all samples (Figure 1c–i).

To further prove the presence of a hydrous phase, a series of ^{31}P{^{1}H} CP MAS NMR experiments were performed. Using this method, only ^{31}P in proximity to ^{1}H is detected and the signal intensity is modulated by the distance and the duration of the contact time. Rhabdophane and monazite are readily distinguished by ^{31}P{^{1}H} CP MAS NMR, as monazite does not contain any water. The CP efficiency peaks at a contact time of 1 ms for rhabdophane, whereas no signals were observed for monazite (Figure 2). ^{1}H MAS NMR spectra (not shown) contain a single resonance with δ_{iso}(^{1}H) ≈ 5 ppm for rhabdophane and no signal above the detection limit from monazite. The observation of a single proton resonance for rhabdophane implies rapid proton exchange between the zeolitic water and the phosphoric acid surface species, in agreement with the proton conduction properties of rhabdophane.[17] Spectra recorded with variable contact time (0.1–5 ms, Figure 2) showed similar behavior for rhabdophane and for a Phoslock sample, as illustrated for LaP100. The maximum intensity of LaP100 is 4% of the maximum of rhabdophane, which is in excellent agreement with the 4.4 w/w % La on Phoslock, and again supports that P_i is captured as rhabdophane.

Local La Environment Monitored by ^{139}La SSNMR and La EXAFS. Further information about the sequestration can be obtained from ^{139}La SSNMR, which gives insight into the La phases formed. ^{139}La QCPMG NMR spectra were recorded for the La model compounds (SI, Figure SI-4) and the Phoslock samples (Figure 3). These spectra, which were recorded at a very high magnetic field to maximize the sensitivity, show a series of so-called spikelets (except for the rhabdophane spectrum which is a powder line shape due to a lack of echoes in the CPMG train) with variable intensity whose manifold traces out the central transition. The ^{139}La NMR parameters extracted from the analysis of these spectra are summarized in Table 2. It is clear that the different La environments have distinct ^{139}La NMR spectra (i.e., parameters) and can be distinguished by solid state ^{139}La NMR.

The spectrum of pure Phoslock shown in Figure 3 cannot be simulated by a simple quadrupole line shape. In this case a Gaussian distribution of the asymmetry parameter, η_Q, broadens the central features enough to allow a fit with a single C_Q value of 44.5 MHz, a δ_{iso}(^{139}La) of 110 ppm, and the

DOI: 10.1021/es506182s
Environ. Sci. Technol. 2015, 49, 4559–4566

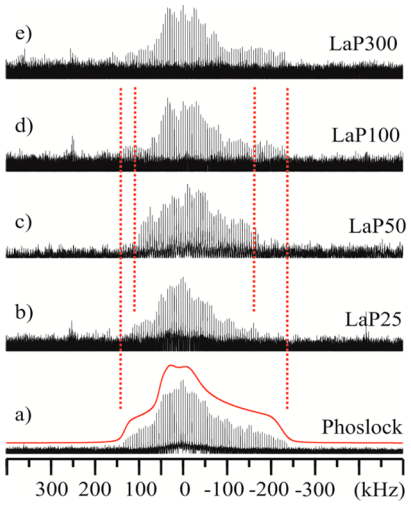

Figure 3. ^{139}La NMR spectra of (a) Phoslock with its simulation in red, (b) LaP25, (c) LaP50, (d) LaP100, and (e) LaP300. End points of the line shapes are marked with vertical dashed lines for convenient comparison.

Table 2. ^{139}La Isotropic Chemical Shifts (δ_{iso}(^{139}La)), Quadrupole Coupling Constant (C_Q), and Asymmetry Parameter (η_Q) Determined for the $LaPO_4$ (Monazite) and Phoslock Spectra in the SI, Figure SI-4

sample	δ_{iso}(^{139}La) (ppm)	C_Q (MHz)	η_Q
$LaPO_4$	36(4)	46.7(10)	0.75(3)
Phoslock	110(10)	44.5(3)	0.80(5)

centroid of η_Q at 0.8 with a sigma of 0.1. In Figure 3 is the calculated powder line shape utilizing these parameters shown. The quadrupole parameters for monazite are more easily extracted as C_Q of 46.7 MHz, η_Q of 0.75, and δ_{iso} of 35.5 ppm. The initial analysis of the rhabdophane spectra is ambiguous due to possible dynamics and site exchange, in agreement with ^{1}H MAS NMR. This could account for the apparent short T_2 (lack of CPMG echoes) which is bolstered by an increased number of echoes upon temperature reduction to −50 °C (data not shown). A washing out of line shape features was also observed by Goward and co-workers in the ^{139}La solid-state NMR of $Li_{3x}La_{2/3-x}TiO_3$ and explained by disorder in both C_Q and η_Q.[37] It is clear from Figure 3 that the ^{139}La NMR spectrum changes as P_i is sequestered from pure Phoslock to a phosphate saturated form (which we conclude above to be dominated by rhabdophane). The most apparent difference is the increase of width of the line shape as the P_i concentration increases. Shown in Figure 3 are dashed vertical lines that illustrate this, where the breadth of the line shape for 25 % and 50 % phosphate loading are narrower than for pure Phoslock, 100 % and 300 % loading. The ^{139}La NMR spectra of LaP100, LaP50, and LaP25 are a superposition of at least two different species. However, it is not possible to extract the relative concentration of these species due to the complexity of these spectra.

EXAFS measurements were performed on three model compounds: rhabdophane, monazite, and lanthanite ($La_2(CO_3)_3{\cdot}8H_2O$),[61,62] and three Phoslock samples (LaP100, LaP100-HA_{500}, and LaP0-HA_{500}). Lanthanite was a pure tracer for bond distances between La and organic substances and LaP0-HA_{500} is Phoslock dispensed in phosphate-free water with 500 μM HA similar to LaP100-HA_{500}. The mean La−O bond

Table 3. Summary of the EXAFS Data (SI, Figure SI-5); Assigned La−O Coordination Number, CN, Bond Distance, d, the Debye−Waller Factor, σ^2, the Amplitude Reduction Factor, S_0^2, and the Threshold Energy, E_0, as Compared to the Reference Value

sample	CN[a]	d/Å	σ^2/Å^2	S_0^2	E_0/eV
$LaPO_4{\cdot}1.4H_2O$	8[b]	2.456(8)	0.0023	0.88	−10.86
$LaPO_4$	9[b]	2.522(6)	0.0196	0.91	−1.17
$La_2(CO_3)_3{\cdot}8H_2O$	10[b]	2.560(4)	0.0094	0.99	−6.43
LaP100	8[b]	2.479(4)	0.0067	0.78	−10.52
LaP100-HA_{500}	9[b]	2.523(3)	0.0074	0.75[b]	−3.24
LaP0-HA_{500}	10[b]	2.555(3)	0.0117	1.06	−2.97

[a]Data from ref 61. [b]Fixed (not refined).

distance increases from 2.45(1)Å for rhabdophane to 2.52(1)Å for monazite (Table 3), which reflects a change in coordination number from eight to nine,[60] and a change toward monazite (detailed results in the SI, Table SI-2 and experimental and fitted spectra in the SI, Figure SI-5). In LaP100 the mean La−O bond distance (2.48(1) Å) matches rhabdophane quite well, which also is in excellent agreement with ^{31}P SSNMR (Figure 1) and further confirms that Phoslock sequester P_i as rhabdophane.

For the Phoslock sample in a phosphate-free solution, LaP0-HA_{500} a mean bond distance of 2.56(1) Å is obtained, which reflects "unreacted" La in the bentonite clay matrix, in agreement with the value for pristine Phoslock. Moreover, this La−O distance agrees well with the 2.57 and 2.50 Å reported earlier for vermiculite in a La(III) nitrate solution and as a powder, respectively,[43] as well as La−O in La-exchanged montmorillonites.[63]

Environmental Relevance of Spectroscopic Knowledge about P_i Sequestration. The ability of Phoslock to sequester P_i was monitored by a model adsorption study, where the SRP concentration remaining in the aqueous phase was determined as a function of DOC. SRP increases as the concentration of DOC increases (0−1000 μM), which indicates that DOC interferes with the binding capacity of Phoslock (Figure 4). At a DOC concentration of 250 μM only 40% of the theoretical capacity of Phoslock is used. Moreover, less than 15% of SRP was removed by Phoslock at DOC concentrations

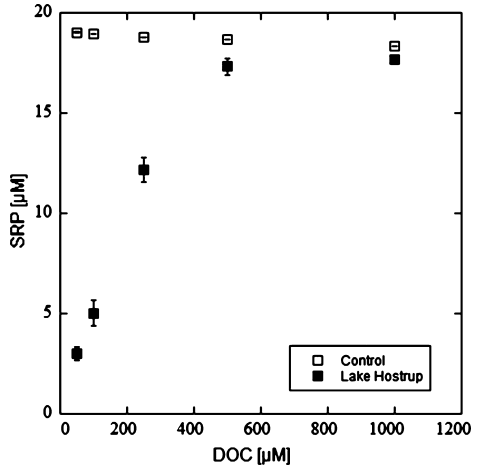

Figure 4. Concentration of soluble reactive phosphorus (SRP) in water, 7 days after Phoslock treatment (■) and controls without Phoslock (□) as a function of DOC concentration.

DOI: 10.1021/es506182s
Environ. Sci. Technol. 2015, 49, 4559−4566

above 600 μM. Efficient P removal (more than 75%) was only observed at DOC concentrations below 100 μM. For a comparison average DOC concentrations of 645 μM[44] and 47 μM[64] were reported for Danish and Dutch lakes, respectively. Thus, this model adsorption study indicates a likely negative influence of DOC of the Phoslock adsorption capacity, supporting earlier results by both Reitzel et al.[14] and Lurling et al.[25] Hence, Phoslock is capable of binding less SRP than theoretical possible in waters containing DOC.

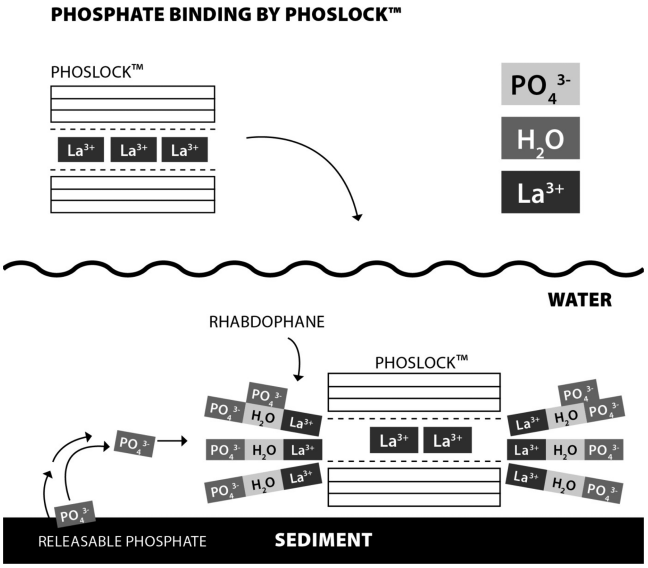

Figure 5. Proposed mechanism for phosphate sequestration on the molecular level based on the results obtained from SSNMR, EXAFS, PXRD, and adsorption studies performed in this study.

Phosphate Sequestration by Phoslock on the Molecular Level. Figure 5 illustrates the mechanism for P_i sequestration based on the results obtained from SSNMR, PXRD, and EXAFS in combination with adsorption studies. Our molecular studies showed that no new La and/or P phases were formed during a Phoslock treatment, and the effect from DOC appears to be kinetic, as proposed by Lürling et al.[25] The bond distance of 2.52(1) Å determined for LaP100-HA_{500} likely reflects a mixture of "unreacted" La and rhabdophane, which also can explain why two La environments were observed by ^{139}La NMR. Although further studies are needed to assess whether the presence of DOC results in a permanent reduction of the Phoslock binding capacity or only in a slower P_i binding kinetic, i.e., longer reaction time than the few hours proposed by Phoslock[22] and the 1 week used in this study.

As the present study shows, Phoslock will sequester P_i as rhabdophane, but this has not previously been structural determined. Rhabdophane is the hydrous La orthophosphate formed at ambient conditions in an aqueous environment and exists in nature as a mineralogical phase, i.e., has very low solubility.[65,66] Monazite is known to exist on a geological time scale, and synthetic monazite is used for storage of radioactive lanthanides,[17,20,67] hence a conversion of rhabdophane to monazite will bind P_i even more strongly. When P_i is captured by Phoslock it is considered biounavailable[6] and no longer a part of the phosphorus cycle in and around the freshwater lakes. La, and thereby Phoslock, is not specificly selective toward binding P_i in forms of orthophosphate, as adsorption studies using one of the following P-compounds: phytic acid, adenosine triphosphate, glucose 6-phosphate, and pyrophosphate showed a reduction of the P_i species by 67(27), 9(15), 0(3), and 19(9) %, respectively, after 1 week (SI, Table SI-3). However, the main species affecting the ecological conditions in the water is orthophosphate, which is the only bioavailable form of P and is found in higher concentrations than organic P in most lake sediments (exceptions are very humic and oligotrophic lakes);[68,69] therefore, the ecological relevance of Phoslock originates from its strong affinity for orthophosphate.

Moreover, this information will be useful for the design of alternative chemical lake restoration products, which do not contain rare/limited resources such as La and/or may impact the lake pH as acidic Al products.

The methodology presented in this study can be successfully applied to further studies of Phoslock and other products invented for environmental remediation, because SSNMR, EXAFS, and PXRD in combination with adsorption studies provide detailed information on how phosphate is sequestered both on the macroscopic and molecular scale, information crucial when designing and optimizing products for environmental remediation.

■ ASSOCIATED CONTENT

Supporting Information

Detailed description of the synthesis procedure for the model compounds ($LaPO_4$ and $LaPO_4{\cdot}1.4H_2O$), TGA data, and ^{139}La SSNMR of the model compounds. Moreover, ^{31}P MAS NMR of the region for the isotropic chemical shift, the EXAFS data and spectra, as well as the crystal structures of monazite and rhabdophane. This material is available free of charge via the Internet at http://pubs.acs.org.

■ AUTHOR INFORMATION

Corresponding Author

*E-mail: ugn@sdu.dk. Phone: +45 6550 4401. Fax: + 45 66158780.

Notes

The authors declare no competing financial interest.

■ ACKNOWLEDGMENTS

The authors gratefully appreciate financial support from the Villum Foundation via the "Villum Young Investigator Programme" (U.G.N. and L.D.) and the CLEAR (Center for Lake Restoration) (L.D. and K.R.). High Field NMR studies were performed at EMSL, a DOE Office of Science User Facility sponsored by the Office of Biological and Environmental Research and located at Pacific Northwest National Laboratory. Portions of this research were carried out at beamline I811, MAX-lab synchrotron radiation source, Lund University, Sweden. Funding for the beamline I811 project was kindly provided by The Swedish Research Council and The Knut och Alice Wallenbergs Stiftelse. Prof. Ingmar Persson, Swedish University of Agricultural Sciences, and Prof. Oleg Antzutkin, University of Luleå, are thanked for fruitful discussions. Valuable comments and suggestions were provided by the anonymous reviewers and the editor, which improved the manuscript.

■ REFERENCES

(1) Spears, B. M.; Dudley, B.; Reitzel, K.; Rydin, E. Geo-Engineering in Lakes-A Call for Consensus. *Environ. Sci. Technol.* **2013**, *47* (9), 3953−3954.

DOI: 10.1021/es506182s
Environ. Sci. Technol. 2015, 49, 4559−4566

(2) Reitzel, K.; Hansen, J.; Andersen, F. Ø.; Hansen, K. S.; Jensen, H. S. Lake Restoration by Dosing Aluminum Relative to Mobile Phosphorus in the Sediment. *Environ. Sci. Technol.* **2005**, *39* (11), 4134−4140.
(3) Gächter, R.; Wehrli, B. Ten Years of Artificial Mixing and Oxygenation: No Effect on the Internal Phosphorus Loading of Two Eutrophic Lakes. *Environ. Sci. Technol.* **1998**, *32* (23), 3659−3665.
(4) Vanderdoes, J.; Verstraelen, P.; Boers, P.; Vanroestel, J.; Roijackers, R.; Moser, G. Lake Restoration with and without Dredging of Phosphorus-Enriched Upper Sediment Layers. *Hydrobiologia* **1992**, *233* (1−3), 197−210.
(5) Lürling, M.; Faassen, E. J. Controlling toxic cyanobacteria: Effects of dredging and phosphorus-binding clay on cyanobacteria and microcystins. *Water Res.* **2011**, *46* (5), 1447−1459.
(6) Robb, M.; Greenop, B.; Goss, Z.; Douglas, G.; Adeney, J. Application of PhoslockTM, an innovative phosphorus binding clay, to two Western Australian waterways: preliminary findings. *Hydrobiologia* **2003**, *494* (1−3), 237−243.
(7) Meis, S.; Spears, B. M.; Maberly, S. C.; O'Malley, M. B.; Perkins, R. G. Sediment amendment with Phoslock® in Clatto Reservoir (Dundee, UK): Investigating changes in sediment elemental composition and phosphorus fractionation. *J. Environ. Manage.* **2012**, *93* (1), 185−193.
(8) Reitzel, K.; Ahlgren, J.; Gogoll, A.; Rydin, E. Effects of aluminum treatment on phosphorus, carbon, and nitrogen distribution in lake sediment: A P-31 NMR study. *Water Res.* **2006**, *40* (4), 647−654.
(9) Lewandowski, J.; Schauser, I.; Hupfer, M. Long term effects of phosphorus precipitations with alum in hypereutrophic Lake Süsser See (Germany). *Water Res.* **2003**, *37* (13), 3194−3204.
(10) Quaak, M.; van der Does, J.; Boers, P.; van der Vlugt, J. A new technique to reduce internal phosphorus loading by in-lake phosphate fixation in shallow lakes. *Hydrobiologia* **1993**, *253* (1−3), 337−344.
(11) Spears, B. M.; Maberly, S. C.; Pan, G.; Mackay, E.; Bruere, A.; Corker, N.; Douglas, G.; Egemose, S.; Hamilton, D.; Hatton-Ellis, T.; Huser, B.; Li, W.; Meis, S.; Moss, B.; Lürling, M.; Phillips, G.; Yasseri, S.; Reitzel, K. Geo-Engineering in Lakes: A Crisis of Confidence? *Environ. Sci. Technol.* **2014**, *48* (17), 9977−9979.
(12) Reitzel, K.; Jensen, H. S.; Egemose, S. pH dependent dissolution of sediment aluminum in six Danish lakes treated with aluminum. *Water Res.* **2013**, *47* (3), 1409−20.
(13) Egemose, S.; Reitzel, K.; Andersen, F. O.; Flindt, M. R. Chemical Lake Restoration Products: Sediment Stability and Phosphorus Dynamics. *Environ. Sci. Technol.* **2010**, *44* (3), 985−991.
(14) Reitzel, K.; Andersen, F. Ø.; Egemose, S.; Jensen, H. S. Phosphate adsorption by lanthanum modified bentonite clay in fresh and brackish water. *Water Res.* **2013**, *47* (8), 2787−2796.
(15) Van Oosterhout, F.; Lürling, M. The effect of phosphorus binding clay (Phoslock®) in mitigating cyanobacterial nuisance: a laboratory study on the effects on water quality variables and plankton. *Hydrobiologia* **2013**, *710* (1), 265−277.
(16) Douglas, G.; Adeney, J.; Robb, M. In *A novel technique for reducing bioavailable phosphorus in water and sediments*; International Association Water Quality Conference on Diffuse Pollution, 1999; pp 517−523.
(17) Jonasson, R. G.; Vance, E. R. DTA Study of the Rhabdophane to Monazite Transformation in Rare-Earth (La-Dy) Phosphates. *Thermochim. Acta* **1986**, *108*, 65−72.
(18) Anfimova, T.; Li, Q.; Jensen, J. O.; Bjerrum, N. J. Thermal Stability and Proton Conductivity of Rare Earth Orthophosphate Hydrates. *Int. J. Electrochem. Sci.* **2014**, *9* (5), 2285−2300.
(19) Ben Moussa, S.; Sobrados, I.; Iglesias, J. E.; Trabelsi-Ayedi, M.; Sanz, J. Synthesis and characterization of the hydrated rare-earth acid diphosphates $LnHP_2O_7$ $3.5H_2O$ (Ln = rare-earth elements). *J. Mater. Chem.* **2000**, *10* (8), 1973−1978.
(20) Glorieux, B.; Matecki, M.; Fayon, F.; Coutures, J. P.; Palau, S.; Douy, A.; Peraudeau, G. Study of lanthanum orthophosphates polymorphism, in view of actinide conditioning. *J. Nucl. Mater.* **2004**, *326* (2−3), 156−162.
(21) Mooney, R. C. L. X-ray Diffraction Study of Cerous Phosphate and Related Crystals 0.1. Hexagonal Modification. *Acta Crystallogr.* **1950**, *3* (5), 337−340.
(22) Ltd., P. W. S. http://www.phoslock.com.au/irm/content/default.aspx (27052014).
(23) Van Oosterhout, F.; Lürling, M. The effect of phosphorus binding clay (Phoslock) in mitigating cyanobacterial nuisance: a laboratory study on the effects on water quality variables and plankton. *Hydrobiologia* **2012**, 1−13.
(24) Reitzel, K.; Lotter, S.; Dubke, M.; Egemose, S.; Jensen, H. S.; Andersen, F. Ø. Effects of Phoslock treatment and chironomids on the exchange of nutrients between sediment and water. *Hydrobiologia* **2012**, *703* (1), 189−202.
(25) Lurling, M.; Waajen, G.; van Oosterhout, F. Humic substances interfere with phosphate removal by lanthanum modified clay in controlling eutrophication. *Water Res.* **2014**, *54*, 78−88.
(26) Pourret, O.; Davranche, M.; Gruau, G.; Dia, A. Rare earth elements complexation with humic acid. *Chem. Geol.* **2007**, *243* (1−2), 128−141.
(27) Tang, J. W.; Johannesson, K. H. Ligand extraction of rare earth elements from aquifer sediments: Implications for rare earth element complexation with organic matter in natural waters. *Geochim. Cosmochim. Acta* **2010**, *74* (23), 6690−6705.
(28) Laws, D. D.; Bitter, H. M.; Jerschow, A. Solid-state NMR spectroscopic methods in chemistry. *Angew. Chem. Int. Ed.* **2002**, *41* (17), 3096−129.
(29) Bryce, D. L.; Bernard, G. M.; Gee, M.; Lumsden, M. D.; Eichele, K.; Wasylishen, R. E. Practical aspects of modern routine solid-state multinuclear magnetic resonance spectroscopy: One-dimensional experiments. *Can. J. Anal. Sci. Spectros.* **2001**, *46* (2), 46−82.
(30) Cade-Menun, B. J. Characterizing phosphorus in environmental and agricultural samples by P-31 nuclear magnetic resonance spectroscopy. *Talanta* **2005**, *66* (2), 359−371.
(31) Kim, J.; Li, W.; Philips, B. L.; Grey, C. P. Phosphate adsorption on the iron oxyhydroxides goethite (α-FeOOH), akaganeite (β-FeOOH), and lepidocrocite (γ-FeOOH): a ^{31}P NMR Study. *Energy Environ. Sci.* **2011**, *4* (10), 4298−4305.
(32) Van Emmerik, T. J.; Sandström, D. E.; Antzutkin, O. N.; Angove, M. J.; Johnson, B. B. 31P solid-state nuclear magnetic resonance study of the sorption of phosphate onto gibbsite and kaolinite. *Langmuir* **2007**, *23* (6), 3205−3213.
(33) Li, W.; Feng, X.; Yan, Y.; Sparks, D. L.; Phillips, B. L. Solid-State NMR Spectroscopic Study of Phosphate Sorption Mechanisms on Aluminum (Hydr)oxides. *Environ. Sci. Technol.* **2013**, *47* (15), 8308−8315.
(34) Yan, Y.; Li, W.; Yang, J.; Zheng, A.; Liu, F.; Feng, X.; Sparks, D. L. Mechanism of Myo-inositol Hexakisphosphate Sorption on Amorphous Aluminum Hydroxide: Spectroscopic Evidence for Rapid Surface Precipitation. *Environ. Sci. Technol.* **2014**, *48* (12), 6735−6742.
(35) Hamaed, H.; Lo, A. Y. H.; Lee, D. S.; Evans, W. J.; Schurko, R. W. Solid-state La-139 and N-15 NMR spectroscopy of lanthanum-containing metallocenes. *J. Am. Chem. Soc.* **2006**, *128* (39), 12638−12639.
(36) Ooms, K. J.; Feindel, K. W.; Willans, M. J.; Wasylishen, R. E.; Hanna, J. V.; Pike, K. J.; Smith, M. E. Multiple-magnetic field 139La NMR and density functional theory investigation of the solid lanthanum(III) halides. *Solid State Nucl. Magn. Reson.* **2005**, *28* (2−4), 125−134.
(37) Spencer, L.; Coomes, E.; Ye, E.; Terskikh, V.; Ramzy, A.; Thangadurai, V.; Goward, G. R. Structural analysis of lanthanum-containing battery materials using 139La solid-state NMR. *Can. J. Chem.* **2011**, *89* (9), 1105−1117.
(38) Herreros, B.; Man, P. P.; Manoli, J.-M.; Fraissard, J. Solid-state 139La NMR investigation of lanthanum-exchanged Y zeolites. *J. Chem. Soc., Chem. Commun.* **1992**, No. 6, 464−466.
(39) Hennig, C.; Reich, T.; Dahn, R.; Scheidegger, A. M. Structure of uranium sorption complexes at montmorillonite edge sites. *Radiochim. Acta* **2002**, *90* (9−11), 653−657.

DOI: 10.1021/es506182s
Environ. Sci. Technol. 2015, 49, 4559−4566

(40) Sun, Y.; Li, J.; Wang, X. The retention of uranium and europium onto sepiolite investigated by macroscopic, spectroscopic and modeling techniques. *Geochim. Cosmochim. Acta* **2014**, *140* (0), 621−643.
(41) Sjostedt, C.; Persson, I.; Hesterberg, D.; Kleja, D. B.; Borg, H.; Gustafsson, J. P. Iron speciation in soft-water lakes and soils as determined by EXAFS spectroscopy and geochemical modelling. *Geochim. Cosmochim. Acta* **2013**, *105*, 172−186.
(42) Hu, J.; Tan, X. L.; Ren, X. M.; Wang, X. K. Effect of humic acid on nickel(II) sorption to Ca-montmorillonite by batch and EXAFS techniques study. *Dalton Trans.* **2012**, *41* (35), 10803−10810.
(43) Jones, D. J.; Roziere, J.; Olivera-Pastor, P.; Rodriguez-Castellon, E.; Jimenez-Lopez, A. Local environment of intercalated lanthanide ions in vermiculite. *J. Chem. Soc., Faraday Trans.* **1991**, *87* (18), 3077−3081.
(44) de Vicente, I.; Jensen, H. S.; Andersen, F. O. Factors affecting phosphate adsorption to aluminum in lake water: Implications for lake restoration. *Sci. Total Environ.* **2008**, *389* (1), 29−36.
(45) Koroleff, F., Determination of phosphorus. In *Methods of seawater analysis*, 2nd ed.; Grasshoff, K. M. E., Kremling, K., Ed.; Verlag Chemie: Weinheim, Germany, 1983; pp 125−139.
(46) Marat, K. *SpinWorks 3.1.8*; University of Manitoba, 2011.
(47) Larsen, F. H.; Jakobsen, H. J.; Ellis, P. D.; Nielsen, N. C. Sensitivity-enhanced quadrupolar-echo NMR of half-integer quadrupolar nuclei. Magnitudes and relative orientation of chemical shielding and quadrupolar coupling tensors. *J. Phys. Chem. A* **1997**, *101* (46), 8597−8606.
(48) O'Dell, L. A.; Rossini, A. J.; Schurko, R. W. Acquisition of ultra-wideline NMR spectra from quadrupolar nuclei by frequency stepped WURST−QCPMG. *Chem. Phys. Lett.* **2009**, *468* (4−6), 330−335.
(49) Bak, M.; Rasmussen, J. T.; Nielsen, N. C. SIMPSON: A General Simulation Program for Solid-State NMR Spectroscopy. *J. Magn. Reson.* **2000**, *147* (2), 296−330.
(50) George, G. N. P, I. J. EXAFSPAK - A suite of computer programs for analysis of X-ray absorption spectra. Stanford Synchrotron Radiation Laboratory: Stanford, CA, 2000.
(51) Solera, J. A.; Garcia, J.; Proietti, M. G.; Sanchez, M. C. L-EXAFS spectra of rare-earth aqueous solutions: detection and study of multielectron transitions. *Physica B* **1995**, *208−209* (0), 71−72.
(52) Zabinsky, S.; Rehr, J.; Ankudinov, A.; Albers, R.; Eller, M. Multiple-scattering calculations of x-ray-absorption spectra. *Phys. Rev. B* **1995**, *52* (4), 2995−3009.
(53) Buissette, V.; Moreau, M.; Gacoin, T.; Boilot, J. P.; Chane-Ching, J. Y.; Le Mercier, T. Colloidal synthesis of luminescent rhabdophane $LaPO_4$: Ln(3+)ct xH_2O (Ln = Ce, Tb, Eu; x approximate to 0.7) nanocrystals. *Chem. Mater.* **2004**, *16* (19), 3767−3773.
(54) Bregiroux, D.; Audubert, F.; Charpentier, T.; Sakellariou, D.; Bernache-Assollant, D. Solid-state synthesis of monazite-type compounds LnPO4 (Ln = La to Gd). *Solid State Sci.* **2007**, *9* (5), 432−439.
(55) Lucas, S.; Champion, E.; Bregiroux, D.; Bernache-Assollant, D.; Audubert, F. Rare earth phosphate powders $RePO_4$ center dot nH_2O (Re= La, Ce or Y) - Part I. Synthesis and characterization. *J. Solid State Chem.* **2004**, *177* (4−5), 1302−1311.
(56) Risskov Sørensen, D.; Nielsen, U. G.; Skou, E. M. Solid state ^{31}P MAS NMR spectroscopy and conductivity measurements on $NbOPO_4$ and H_3PO_4 composite materials. *J. Solid State Chem.* **2014**, *219* (0), 80−86.
(57) Dithmer, L., Reitzel, K., Nielsen, U. G. Unpublished.
(58) Ben Moussa, S.; Ventemillas, S.; Cabeza, A.; Gutierrez-Puebla, E.; Sanz, J. Structure of trihydrated rare-earth acid diphosphates LnHP2O7·3H2O (Ln=La, Er). *J. Solid State Chem.* **2004**, *177* (6), 2129−2137.
(59) Sandström, D. E.; Jarlbring, M.; Antzutkin, O. N.; Forsling, W. A Spectroscopic Study of Calcium Surface Sites and Adsorbed Iron Species at Aqueous Fluorapatite by Means of 1H and 31P MAS NMR. *Langmuir* **2006**, *22* (26), 11060−11064.
(60) Shand, C. A.; Cheshire, M. V.; Bedrock, C. N.; Chapman, P. J.; Fraser, A. R.; Chudek, J. A. Solid-phase 31P NMR spectra of peat and mineral soils, humic acids and soil solution components: influence of iron and manganese. *Plant Soil* **1999**, *214* (1−2), 153−163.
(61) Hellenbrandt, M. The Inorganic Crystal Structure Database (ICSD)—Present and Future. *Crystallogr. Rev.* **2004**, *10* (1), 17−22.
(62) Lundberg, D.; Persson, I.; Eriksson, L.; D'Angelo, P.; De Panfilis, S. Structural Study of the N,N′-Dimethylpropyleneurea Solvated Lanthanoid(III) Ions in Solution and Solid State with an Analysis of the Ionic Radii of Lanthanoid(III) Ions. *Inorg. Chem.* **2010**, *49* (10), 4420−4432.
(63) Trillo, J.; Alba, M.; Castro, M.; Munoz, A.; Poyato, J.; Tobias, M. Local environment of lanthanum ions in montmorillonite upon heating. *Clay Miner.* **1992**, *27* (4), 423−434.
(64) De Lange, H. J. The attenuation of ultraviolet and visible radiation in Dutch inland waters. *Aquatic Ecol.* **2000**, *34* (3), 215−226.
(65) Lucas, S.; Champion, E.; Bernache-Assollant, D.; Leroy, G. Rare earth phosphate powders $RePO_4$ nH_2O (Re = La, Ce or Y) II. Thermal behavior. *J. Solid State Chem.* **2004**, *177* (4−5), 1312−1320.
(66) Firsching, F. H.; Brune, S. N. Solubility Products of the Trivalent Rare-Earth Phosphates. *J. Chem. Eng. Data* **1991**, *36* (1), 93−95.
(67) Oelkers, E. H.; Montel, J. M. Phosphates and nuclear waste storage. *Elements* **2008**, *4* (2), 113−116.
(68) Ahlgren, J.; Reitzel, K.; Danielsson, R.; Gogoll, A.; Rydin, E. Biogenic phosphorus in oligotrophic mountain lake sediments: Differences in composition measured with NMR spectroscopy. *Water Res.* **2006**, *40* (20), 3705−3712.
(69) Joniak, T. The structure of phosphorus compounds in mid-forest humic lakes. *Ocean Hydrobiol. Stud.* **2010**, *39*, 105.

DOI: 10.1021/es506182s
Environ. Sci. Technol. 2015, 49, 4559−4566